Letter

Driving a magnetic texture by magnon currents

M. Vogel,[1,2] B. Zimmermann [1] J. Wild [1] F. Schwarzhuber [1] C. Mewes,[3] T. Mewes [3]
J. Zweck [1] and C. H. Back [1,4]

[1]*Department of Physics, Regensburg University, 93053 Regensburg, Germany*
[2]*Institute for Materials Science, Kiel University, Kaiserstraße 2, 24143 Kiel, Germany*
[3]*Department of Physics and Astronomy, The University of Alabama, Tuscaloosa, Alabama 35487, USA*
[4]*Department of Physics, Technical University Munich, 85748 Garching, Germany*

Thermally induced spin dynamics in solids have sparked broad interest in both fundamental physics and spintronic applications. As theoretically proposed, thermally excited magnons created by temperature gradients can be used to manipulate spin textures such as topological magnetic solitons. However, so far, the effectiveness of such thermomagnonic torques remained a problem in practice. Here, the dynamics of magnetic vortex cores in thin ferromagnetic platelets driven by thermomagnonic torques are investigated using high-resolution Lorentz transmission electron microscopy. Large deflections of the magnetic vortex core transverse to the direction of the temperature gradient are observed. A generalized Thiele equation model is used to identify the magnitude of the contribution of the involved torques. Our results pave the way for the manipulation of magnetic domains on the nanoscale by thermomagnonic currents and provide insights into the interplay of temperature and spin.

In the field of spin caloritronics [1,2], the interaction between heat, charge, and spin currents is currently being investigated from the perspective of fundamental physics and spintronic applications. It is motivated by physical effects including spin-dependent thermopower [3], spin-dependent Peltier effect [4], thermal spin transfer torque [5], spin [5,6] and anomalous Nernst effects [7,8], spin Seebeck tunneling [4], and the thermal Hall effect [9] to name a few.

In general, a temperature gradient $\vec{\nabla}T$ is the driving force for the diffusive motion of (quasi)particles; phonons, magnons, and electrons in the solid state move from the hot to the cold region.

In a ferromagnetic insulator, the diffusion of magnons in a temperature gradient transports angular momentum which can, in turn, drive magnetic textures. Pure thermomagnonic spin torques couple the magnetic moments to a temperature gradient even in the absence of electric charge currents [10,11]. Thermally excited magnons created by large temperature gradients (in the order of K/nm) were recently proposed to be used to efficiently manipulate magnetic structures [12,13] and, indeed, it has been shown that magnetic domain walls can be thermally driven in yttrium iron garnet ($Y_3Fe_5O_{12}$, YIG) [14]. Furthermore, the discussion of pure thermomagnonic torques has recently become the focus of studies in insulating ferrimagnets, such as YIG [14,15], and other magnetic insulators, such as $BaFe_{11.79}Sc_{0.16}Mg_{0.05}O_{19}$ [16] and Cu_2OSeO_3 [17]. In the helimagnetic multiferroic Cu_2OSeO_3, thermally driven ratchet motion of a skyrmion lattice was observed in the presence of a temperature gradient [18,19]. This motion is caused by the topological magnon Hall effect and was later quantified in dependence of the magnitude of an applied temperature gradient [20] and thus the magnitude of the applied thermally driven magnon current.

In metals, in addition to the thermally induced magnon diffusion, the temperature gradient also leads to a thermally induced electron current which in ferromagnets is spin polarized. This spin current can exert a torque on a spin texture, leading to temperature gradient induced spin texture dynamics due to conservation of total angular momentum [21,22].

When compared to topologically trivial spin textures, vortexlike topological spin textures such as magnetic skyrmions [23–25] and vortex cores [26–29] require lower spin current densities to be actuated [25,30–33]. The manipulation of such particles is at the heart of spintronics and is one of the key challenges in the development of high-density magnetic storage and logic devices [23]. Traditionally, the manipulation of such topological solitons is achieved by spin-polarized electric charge currents due to the application of an electrical potential [34].

In this paper, the emphasis is on thermal magnon driven spintexture dynamics in the ferromagnetic metal permalloy (Py). Besides the ease of thin-film preparation by sputter deposition, ferromagnetic metals also bring the possibility of all electric readout of the magnetic texture [35,36]. While thermal magnon driven domain-wall motion has been theoretically proposed [37,38], the effectiveness of such thermomagnonic torques remained a problem in practice.

To achieve large temperature gradients, a SiN-membrane platform is used. A gold meander heater is placed on a 30-nm-thin SiN membrane close to the 200-μm-thick Si frame, which acts as a heat sink (see Fig. 1). In this geometry, temperature gradients of up to 0.12 K/nm can be achieved by applying a heating voltage U_{heat} between 0 and 0.27 V to the Au meander. A 20-nm-thick permalloy (Py) disk with a diameter of 2 μm is placed in between the heater and the edge of the membrane and subjected to the large temperature gradients. The magnetic structure inside the disk is in its
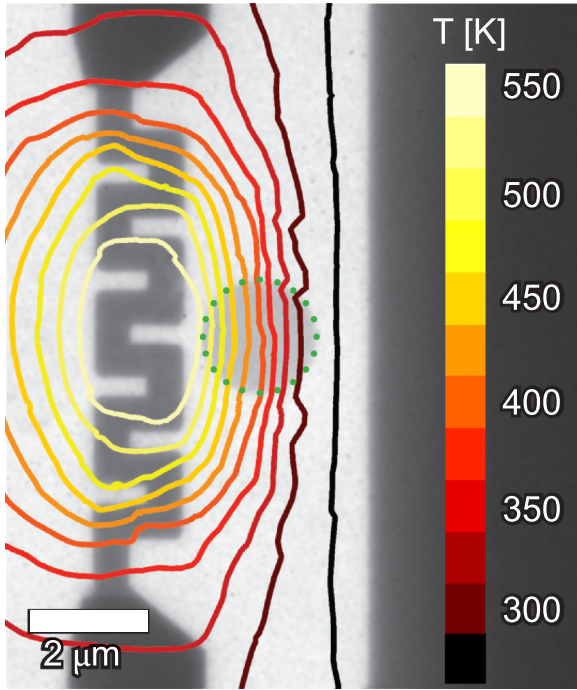
FIG. 1. TEM image of the used sample geometry. The meander heater can be seen on the left of the SiN-membrane (light contrast). The Py disk (green dotted line) is placed between the heater and the frame of the membrane (dark contrast) on the right, which acts as heat sink. The isothermals of the temperature distribution calculated by 3D FEM simulation is overlaid with the color temperature scale on the right. In the region of the Py disk, the temperature gradient $\vec{\nabla} T$ is along the x axis.

energetic ground state, a magnetic vortex structure [39,40]. It is characterized by an in-plane curling magnetization and an out-of-plane core. The sense of rotation of the vortex defines the chirality $c = \pm 1$. The chirality for all measurements is $c = 1$, resulting in a bright contrast in combination with a negative defocus. Additionally, the magnetization direction of the perpendicularly magnetized vortex core (up or down) defines the polarity $p = \pm 1$. A magnetic vortex core in a 20-nm-thick permalloy (Py) disk with a diameter of $2 \, \mu m$ is subjected to the large temperature gradients. The motion of the vortex core is observed by high-resolution Lorentz transmission electron microscopy (L-TEM) using a FEI Tecnai F30. The sample plane is perpendicular to the optical axis of the beam and allows imaging of the in-plane component of the magnetization. The contrast of a defocused image ($\Delta f = -10 \, \mu m$) is projected onto a phosphorescence screen and images are acquired via a CCD camera. The combination of the chosen chirality $c = 1$ and a negative defocus Δf lead to a bright-dot-like (see Supplemental Material [41]) contrast in the middle of the Py disk who's dynamics are investigated. A dependence of the lateral movement orthogonal to the applied temperature gradient and the vortex core polarity is demonstrated. The driving force for this is identified as pure thermomagnonic torque by a combination of analytic calculations and micromagnetic simulations.

Due to the well established description of their dynamics [40,42], energetic stability due to topological protection [43], and easy experimental accessibility as magnetic ground states found in laterally confined magnetic thin films with closed flux domain structure [44], magnetic vortices are an ideal toy system to investigate thermomagnonic torques. The magnetic vortex structure [39,40] is characterized by an in-plane curling magnetization. Its sense of rotation defines the chirality $c = \pm 1$. Additionally, the magnetization direction of the perpendicularly magnetized vortex core (up or down) defines the polarity $p = \pm 1$. For disk shaped soft magnetic elements this magnetization structure causes flux closure of the in-plane magnetization leaving only the out-of-plane core with a size of 10 nm to 30 nm to generate a small stray field [45]. In this case the magnetization dynamics can be described within the framework of micromagnetic simulations or an analytic solution based on the Thiele equation $\vec{F} + \vec{G} \times \vec{V} + \alpha \hat{D} \vec{V} = 0$. Here $\vec{V} = d\vec{R}/dt$ is the velocity of the vortex core, with time t and position $\vec{R} = (x(t), y(t))$ of the vortex core. $\vec{G} = G_0 \hat{e}_z$ is the gyrovector and can be represented with the components of the antisymmetric gyrotensor $G_0 = -2\pi p t M_s / \gamma$ [40,46]. M_s is the saturation magnetization, γ the gyromagnetic ratio, and $\hat{D}$ is the dissipation tensor. It is diagonal with $D_{xx} = D_{zz} = D_0$ and $D_{zz} = 0$ [46]. α is the Landau-Lifshitz damping constant for the magnetization dynamics. In the case of an applied temperature gradient along the x direction, $\vec{\nabla} T = \frac{\partial T}{\partial x} \hat{x}$, the force vector ($\vec{F}$) includes the force due to the stray field ($\vec{F}_{st}$), pure thermomagnonic torques ($\vec{F}_m$), spin transfer torques via electric currents $\vec{F}_c$, and thermal fluctuations ($\vec{F}_{fl}$). Using the superposition principle, the total force can be expressed by $\vec{F} = \vec{F}_{st} + \vec{F}_m + \vec{F}_c + \vec{F}_{fl}$. The force due to the stray field $\vec{F}_{st}$ can be derived by assuming a parabolic potential with stiffness constant [40] $\tilde{\kappa}$: $\vec{F}_{st} = -m\omega_r^2 x \hat{e}_x - m\omega_r^2 y \hat{e}_y$ with $\tilde{\kappa} = \frac{1}{2} m \omega_r^2$. The three last terms in the sum of the forces describe the forces acting on the magnetic vortex core due to the application of a thermal gradient. Here, the focus lies on the forces due to pure thermomagnonic torques ($\vec{F}_m$). The resulting movements due to thermally induced charge currents and thermal fluctuations can be neglected for the experimentally accessible temperature gradients (see Supplemental Material [41]). To include a pure thermomagnonic torque, we follow the approach chosen by Tatara [38] where, for the case of a magnon current flowing along the x axis, the resulting force in the extended Thiele equation takes the following form:

$$\vec{F}_m = \frac{\pi k_B^2 J a^4}{13 \hbar^3 v_m^2} t_{Py} \frac{T}{\alpha} \frac{\partial T}{\partial x} \vec{G} \times \hat{x}. \qquad (1)$$

t_{Py} is the thickness of the permalloy sample, J the exchange constant, a the lattice parameter, v_m is the effective velocity (group velocity) of the magnon, and k_B the Boltzmann constant. The effective magnon velocity can be estimated via $v_m = \frac{2A}{(l_{ex} \mu_0 M_s / \gamma)}$, with A the exchange constant. This gives for permalloy a value of approximately 1000 m/s. To calculate the final core deflection due to the pure magnon transfer torque, the generalized Thiele equation can be solved for a stationary condition, i.e., $\frac{dx}{dt} = \frac{dy}{dt} = 0$. Under this condition,
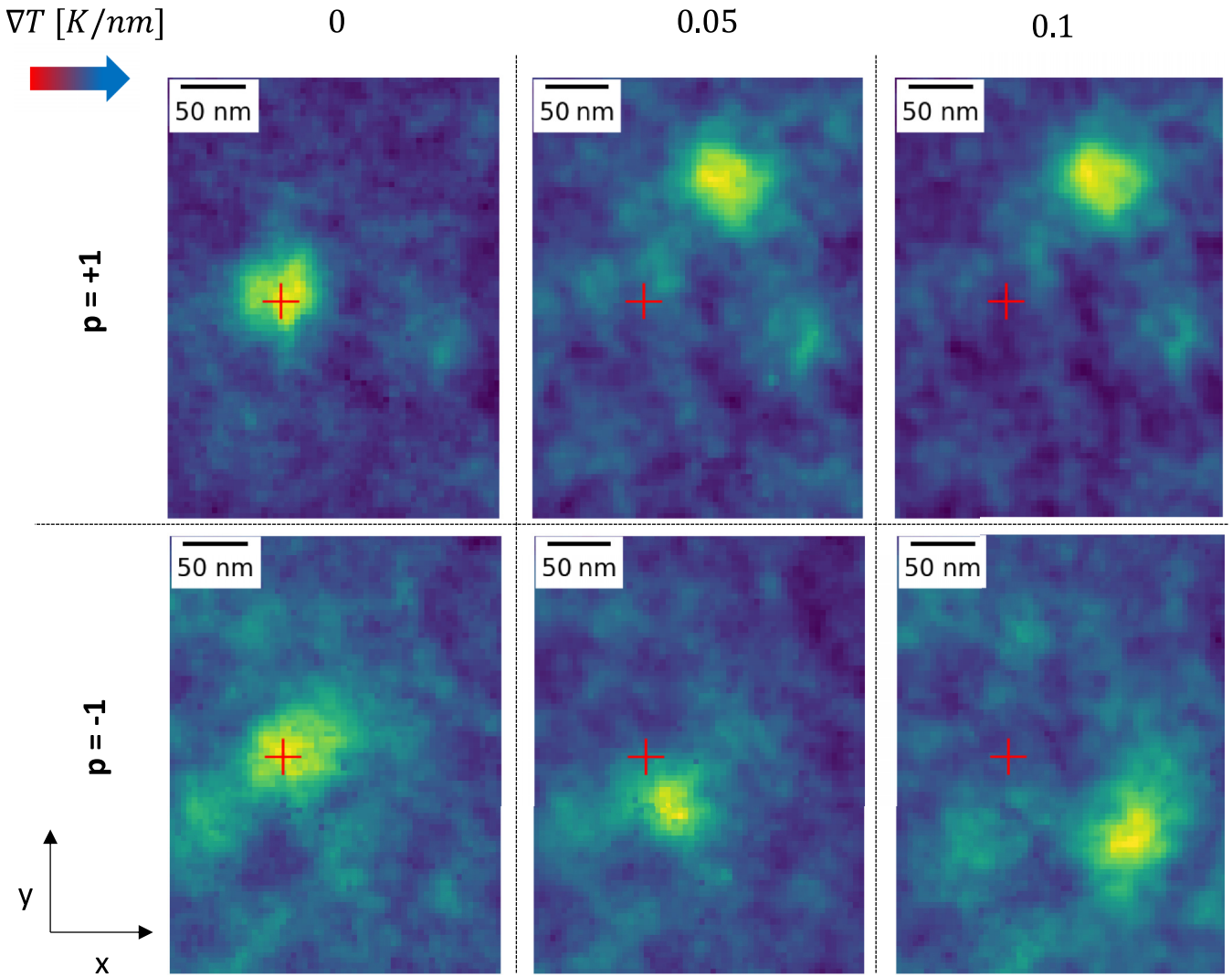
FIG. 2. L-TEM measurements of the vortex core displacement for different combinations of applied temperature gradients $\vec{\nabla}T$ and vortex core polarities $p = +1$ (top row) and $p = -1$ (bottom row). The direction of $\vec{\nabla}T$ is along the x direction (indicated by the arrow), with the hot side being on the left. For $p = +1$, the vortex core shifts to positive Δy with increasing $\vec{\nabla}T$ due to TMSTT. For a reversed polarity $p = -1$, the vortex core shifts to negative values Δy with increasing $\vec{\nabla}T$. In both cases, a shift in positive x direction is observed due to the partial demagnetization of the Py disk on the hot side.

the final core deflection is given by

$$\begin{pmatrix} \Delta x_{\text{end}}^m \\ \Delta y_{\text{end}}^m \end{pmatrix} = \frac{1}{\Gamma^2 - \omega^2} \begin{pmatrix} -\Gamma v_{mx} + p\omega v_{my} \\ p\omega v_{mx} - \Gamma v_{my} \end{pmatrix}$$

$$= \begin{pmatrix} 0 \\ -\frac{p\omega}{\Gamma^2 + \omega^2} \frac{2Ja^2}{\hbar} j_m \end{pmatrix}. \qquad (2)$$

Γ characterizes the damping factor of the vortex motion. It is given by $\Gamma = -\frac{pG_0 m\omega_r^2}{G_0^2 + D_0^2\alpha^2}$ [46]. $\omega = -\frac{pG_0 m\omega_r^2}{G_0^2 + D_0^2\alpha^2}$ is the free frequency of the spiral vortex motion that the exited vortex performs around its equilibrium position in the absence of current and field.

For a finite temperature gradient along the x direction, $\vec{F}_m$ results in an orthogonal motion of the vortex core. Similar to charge current driven spin transfer torque (STT), the sign of the motion depends on the sign of the vortex core polarity p due to the even dependency of the antisymmetric gyrotensor

on p. In the experiment, where one side of the sample is heated to create a large temperature gradient, one has to take into account that the hot side of the disk will reach temperatures high enough to decrease the saturation magnetization M_s in a small region on the hot side of the sample. The resulting gradient of the saturation magnetization leads to a motion of the vortex core along the direction of $\vec{\nabla}T$ as shown in Ref. [47]. To estimate the movement caused by the reduction of M_s, we performed micromagnetic simulations (see Supplemental Material [41]). This motion is independent of the polarization p of the core.

To experimentally observe the motion due to thermo-magnonic torques, large temperature gradients of the order of 0.1 K/nm are needed. To realize temperature gradients of this order of magnitude, the Py disk is placed between the meander heater on the left (see Fig. 1) and the edge of the SiN-membrane (dark contrast on the right). The z dimension of the frame (200 μm) is infinitely thick compared to the
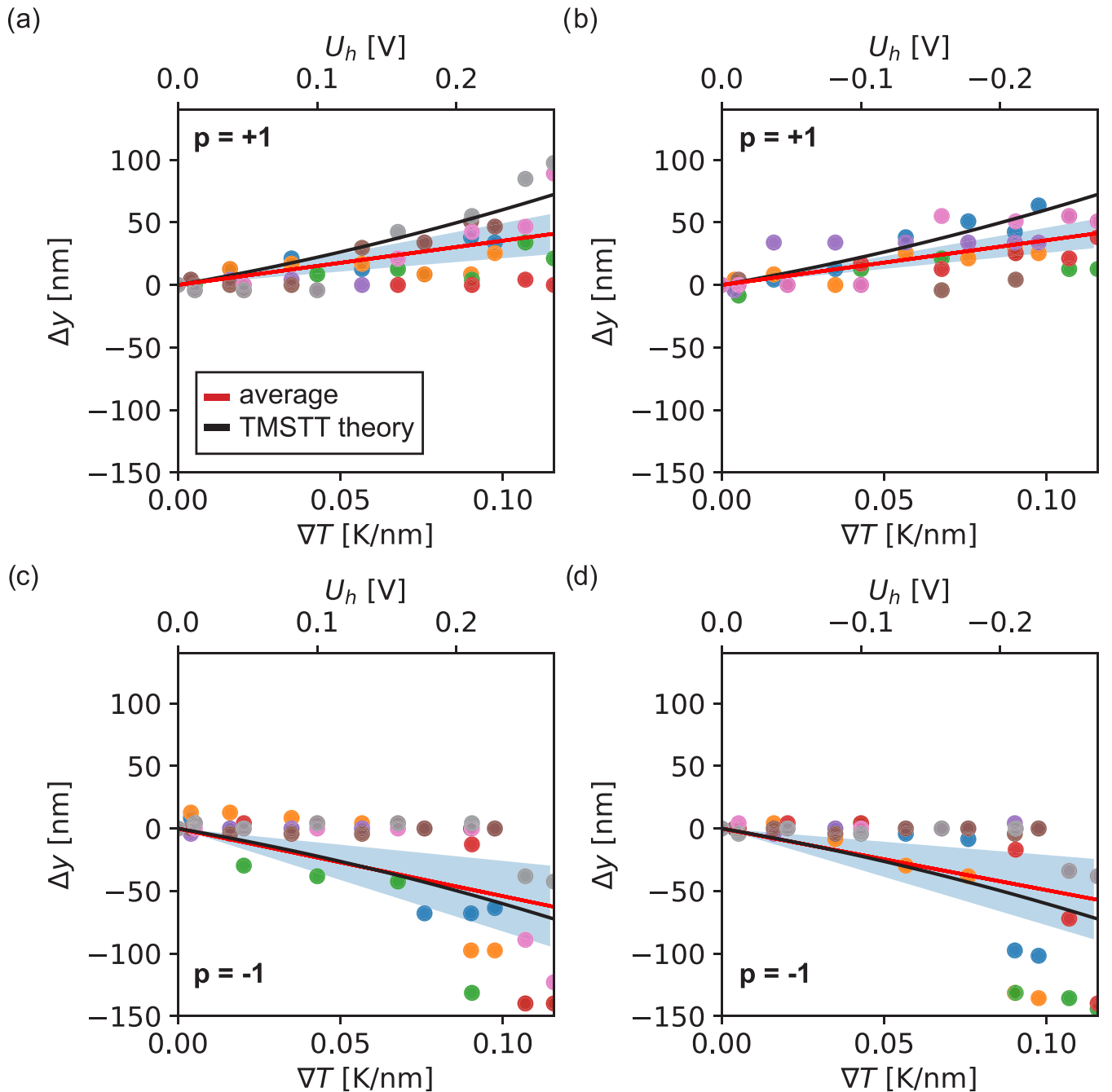
FIG. 3. Statistic plots of the vortex core shift. Δy is perpendicular to the applied temperature gradient. The observed values are shown as a scatter plot with the color indicating each measurement series versus the applied temperature gradient (lower x axis). The corresponding heating voltages U_{heat} are shown in the top x axis. A linear fit is applied to the data points (red) with the lower and upper standard error limits shown in blue. The theoretical values obtained with an extended Thiele equation model are indicated in black. (a) For a positive polarity $p = +1$, the core shifts to positive Δy values. (b) The same shift is observed if the sign of U_{heat} is reversed. (c) If the polarity is reversed, so is the direction of the vortex core shifts. (d) The same shifts are observed for negative values of U_{heat}. The motion of the vortex core calculated by the extended Thiele model is shown in black.

membrane itself (30 nm) and serves as a heat sink. The temperature distribution across the sample plane is calculated by 3D finite element simulations using the COMSOL package. The resulting temperature gradients were experimentally verified by additional electrical measurements on a similar sample with a resistance temperature probe in place of the Py disk (see Supplemental Material [41]).

To measure the dependence of the vortex core movement Δx and Δy on the temperature gradient, different voltages $U_{\text{heat}} = 0$ V to 0.27 V are applied to the heater, resulting in $\vec{\nabla}T$ of up to 0.1 K/nm. A series of three images for each polarity is taken at increasing values of U_{heat}, as shown in Fig. 2. The chirality is kept at $c = 1$ for all measurements to avoid changes to the spin-polarized thermomagnonic current

due to changes in the in-plane magnetic texture of the vortex. The direction of the temperature gradient is, as indicated by the arrow, along the x direction, with the hot side being on the left. The position of the vortex core for $\vec{\nabla}T = 0$ (vortex core in equilibrium state) is indicated in all images by a red cross. For this case, both shifts, parallel and orthogonal to $\vec{\nabla}T$, are equal to zero. The polarity of the vortex core can be initiated by demagnetizing the sample with a large magnetic field perpendicular to the sample in the positive or negative z direction. For a polarity of $p = +1$ (see Fig. 2, upper row) the vortex core shifts to positive values of Δy. The shift increases with higher values of $\vec{\nabla}T$. If the polarity is switched to $p = -1$, the direction of the shift in the y direction also changes signs, causing a downward movement of the vortex core as shown in Fig. 2 (lower row). There is no change in contrast of the core due to the same chirality and the measurement not being sensitive to the out-of-plane component of the magnetization which is switched. This agrees with the theoretical predictions of the analytical calculation based on the Thiele equation. In both cases, the shift along the direction of $\vec{\nabla}T$ is from the hot to the cold side (independent of p) due to a slight decrease of M_s in a region at the hot side of the Py disk. However, there is a small deviation of the magnitude of the shifts from $p = +1$ to $p - 1$. This is caused by the local energy landscape created by pinning centers, inevitable for such thin permalloy films deposited on the relatively rough surface of the SiN membrane. To further investigate this behavior and rule out the possibility of the change of direction of Δy, being solely due to local energy landscape (local pinning), a series of 256 measurements, with samples prepared in the same manner, was performed. The positions of the vortex cores were automatically tracked by the Laplacian of the Gaussian method [48] and the relative shifts Δx and Δy from the equilibrium position at the beginning of each image series were determined. The results are shown in Fig. 3. For a polarity $p = +1$ [see Fig. 3(a)], the shifts are again to positive values of Δy. The influence of the local energy landscape due to local pinning centers and the limited experimental lateral resolution becomes visible in plateaus of Δy, especially for small values of $\vec{\nabla}T$. In this case, the magnitude of the thermomagnonic spin torque needs to overcome a threshold value due to the local pinning. In most measurements, the observed shifts after overcoming this threshold show a linear dependence on $\vec{\nabla}T$. In some cases, the movement ends in a new local minimum causing a slight deviation from the linear dependence. No significant shifts to negative values are observed if the resolution limit is taken into account. Due to the almost linear dependence of the theoretically predicted shift due to the thermomagnonic spin torque, the observed values of Δy are fitted by a linear regression (red line). The statistical error limits of the fit are shown as blue area. Compared to the theoretically predicted Δy (indicated as solid black lines), the observed

values in the Lorentz-TEM measurements are slightly smaller, most likely due to the fact that pinning centers have not been taken into account in the extended Thiele model. Due to the electric current passing through the heater, an additional parasitic Oersted field is created. This field is mainly perpendicular to the sample plane due to the sample geometry. The field was also simulated by COMSOL simulations. The out-of-plane component is below $B_z < 10$ mT and does not cause a lateral motion of the magnetic vortex core. The in-plane component is about two orders of magnitude smaller and can be neglected as well. To further rule out any effect of the generated Oersted field, the same measurement series were performed for reversed values of U_{heat}. For negative values and the same polarity $p = +1$, the same overall behavior is observed, as shown in Fig. 3(b), ruling out an influence of the Oersted field created by the current passing through the heater. If the polarity is reversed to polarity $p = -1$, the vortex core shifts, as previously predicted, to negative values of Δy [see Fig. 3(c)]. Taking all data points into account, the average movement determined by the fit is again slightly below the theoretical predictions due to the effect of local pinning centers. As for polarity $p = +1$, the reversal of U_{heat} from positive to negative values does not change the overall direction of Δy [see Fig. 3(d)].

In conclusion, we demonstrate the action of a thermally induced magnon current on a localized magnetic texture, namely, a magnetic vortex. Its experimentally resolved movement in an applied temperature gradient $\vec{\nabla}T$ matches the theoretical predictions. A reversal of the polarization of the vortex core is accompanied by a change of the direction of Δy, the component of the movement orthogonal to $\vec{\nabla}T$. The magnitude of the observed shifts Δy is on average slightly below the theoretically predicted results, which is most likely caused by local pinning of the vortex core typical for thin Py films. Further, the shift Δy perpendicular to the applied temperature gradient scales with the effective magnon velocity as shown in Fig. 3. The effective magnon velocity for a 20-nm-thick Py film is estimated as 1900 m/s [49] and 2200 m/s [50]. By taking the linear regression, calculated from the experimental data (red line), it is possible to scale the effective magnon velocity by the fitted slope: $v_{\text{mexp}} = 2200$ m/s $\pm$ 1900 m/s. This is by no means a precise measurement of v_m but serves as a sanity check. A reversal of the electric current direction inside the heater does not change the overall behavior of the movement. An influence of magnetic fields induced by the electric current can be excluded. A similar-sized movement parallel to $\vec{\nabla}T$ is observed, independent of the polarity and the direction of the current inside the heater. This shift can be explained by the partial reduction of the saturation magnetization on the hot side of the Py element, as shown by a combination of micromagnetic and analytic calculations.

[1] G. E. W. Bauer, E. Saitoh, and B. J. Van Wees, Spin caloritronics, Nat. Mater. **11**, 391 (2012).

[2] G. E. W. Bauer, A. H. MacDonald, and S. Maekawa, Spin caloritronics, Solid State Commun. **150**, 459 (2010).

[3] A. Slachter, F. L. Bakker, J. P. Adam, and B. J. Van Wees, Thermally driven spin injection from a ferromagnet into a non-magnetic metal, Nat. Phys. **6**, 879 (2010).

[4] J. C. Le Breton, S. Sharma, H. Saito, S. Yuasa, and R. Jansen, Thermal spin current from a ferromagnet to silicon by Seebeck spin tunnelling, Nature (London) **475**, 82 (2011).

[5] M. Hatami, G. E. W. Bauer, Q. Zhang, and P. J. Kelly, Thermal Spin-Transfer Torque in Magnetoelectronic Devices, Phys. Rev. Lett. **99**, 066603 (2007).

[6] S. Meyer, Y.-T. Chen, S. Wimmer, M. Althammer, T. Wimmer, R. Schlitz, S. Geprägs, H. Huebl, D. Ködderitzsch, H. Ebert, G. E. W. Bauer, R. Gross, and S. T. B. Goennenwein, Observation of the spin Nernst effect, Nat. Mater. **16**, 977 (2017).

[7] S. Y. Huang, W. G. Wang, S. F. Lee, J. Kwo, and C. L. Chien, Intrinsic Spin-Dependent Thermal Transport, Phys. Rev. Lett. **107**, 216604 (2011).

[8] Y. Pu, E. Johnston-Halperin, D. D. Awschalom, and J. Shi, Anisotropic Thermopower and Planar Nernst Effect in Ga1-xMnxAs Ferromagnetic Semiconductors, Phys. Rev. Lett. **97**, 036601 (2006).

[9] S. Park, N. Nagaosa, and B. J. Yang, Thermal hall effect, spin nernst effect, and spin density induced by a thermal gradient in collinear ferrimagnets from magnon-phonon interaction, Nano Lett. **20**, 2741 (2020).

[10] A. A. Kovalev and Y. Tserkovnyak, Thermoelectric spin transfer in textured magnets, Phys. Rev. B **80**, 100408(R) (2009).

[11] A. A. Kovalev and Y. Tserkovnyak, Magnetocaloritronic nanomachines, Solid State Commun. **150**, 500 (2010).

[12] D. Hinzke and U. Nowak, Domain Wall Motion by the Magnonic Spin Seebeck Effect, Phys. Rev. Lett. **107**, 027205 (2011).

[13] L. Kong and J. Zang, Dynamics of an Insulating Skyrmion Under a Temperature Gradient, Phys. Rev. Lett. **111**, 067203 (2013).

[14] W. Jiang, P. Upadhyaya, Y. Fan, J. Zhao, M. Wang, L. T. Chang, M. Lang, K. L. Wong, M. Lewis, Y. T. Lin, J. Tang, S. Cherepov, X. Zhou, Y. Tserkovnyak, R. N. Schwartz, and K. L. Wang, Direct Imaging of Thermally Driven Domain Wall Motion in Magnetic Insulators, Phys. Rev. Lett. **110**, 177202 (2013).

[15] S. Bhagat, H. Lessoff, C. Vittoria, and C. Guenzer, Spin-wave resonance studies on chemical vapor deposited YIG films, Phys. Status Solidi (a) **20**, 731 (1973).

[16] X. Yu, M. Mostovoy, Y. Tokunaga, W. Zhang, K. Kimoto, Y. Matsui, Y. Kaneko, N. Nagaosa, and Y. Tokura, Magnetic stripes and skyrmions with helicity reversals, Proc. Natl. Acad. Sci. USA **109**, 8856 (2012).

[17] S. Seki, X. Z. Yu, S. Ishiwata, and Y. Tokura, Observation of skyrmions in a multiferroic material, Science **336**, 198 (2012).

[18] M. Mochizuki, X. Y. Yu, S. Seki, N. Kanazawa, W. Koshibae, J. Zang, M. Mostovoy, Y. Tokura, and N. Nagaosa, Thermally driven ratchet motion of a skyrmion microcrystal and topological magnon Hall effect, Nat. Mater. **13**, 241 (2014).

[19] C. Gong, Y. Zhou, and G. Zhao, Dynamics of magnetic skyrmions under temperature gradients, Appl. Phys. Lett. **120**, 052402 (2022).

[20] X. Yu, F. Kagawa, S. Seki, M. Kubota, J. Masell, F. S. Yasin, K. Nakajima, M. Nakamura, M. Kawasaki, N. Nagaosa, and Y. Tokura, Real-space observations of 60-nm skyrmion dynamics in an insulating magnet under low heat flow, Nat. Commun. **12**, 5079 (2021).

[21] H. Kohno, Y. Hiraoka, M. Hatami, and G. E. W. Bauer, Microscopic calculation of thermally induced spin-transfer torques, Phys. Rev. B **94**, 104417 (2016).

[22] J. Torrejon, G. Malinowski, M. Pelloux, R. Weil, A. Thiaville, J. Curiale, D. Lacour, F. Montaigne, and M. Hehn, Unidirectional Thermal Effects in Current-Induced Domain Wall Motion, Phys. Rev. Lett. **109**, 106601 (2012).

[23] A. Fert, V. Cros, and J. Sampaio, Skyrmions on the track, Nat. Nanotechnol. **8**, 152 (2013).

[24] W. Jiang, P. Upadhyaya, W. Zhang, G. Yu, M. B. Jungfleisch, F. Y. Fradin, J. E. Pearson, Y. Tserkovnyak, K. L. Wang, O. Heinonen, S. G. E. te Velthuis, and A. Hoffmann, Magnetism. Blowing magnetic skyrmion bubbles, Science **349**, 283 (2015).

[25] F. Jonietz, S. Mühlbauer, C. Pfleiderer, A. Neubauer, W. Münzer, A. Bauer, T. Adams, R. Georgii, P. Böni, R. A. Duine, K. Everschor, M. Garst, and A. Rosch, Spin transfer torques in MnSi at ultralow current densities, Science **330**, 1648 (2010).

[26] S. Kasai, Y. Nakatani, K. Kobayashi, H. Kohno, and T. Ono, Current-Driven Resonant Excitation of Magnetic Vortices, Phys. Rev. Lett. **97**, 107204 (2006).

[27] M. Bolte, G. Meier, B. Krüger, A. Drews, R. Eiselt, L. Bocklage, S. Bohlens, T. Tyliszczak, A. Vansteenkiste, B. Van Waeyenberge, K. W. Chou, A. Puzic, and H. Stoll, Time-Resolved X-Ray Microscopy of Spin-Torque-Induced Magnetic Vortex Gyration, Phys. Rev. Lett. **100**, 176601 (2008).

[28] K. Yamada, S. Kasai, Y. Nakatani, K. Kobayashi, H. Kohno, A. Thiaville, and T. Ono, Electrical switching of the vortex core in a magnetic disk, Nat. Mater. **6**, 270 (2007).

[29] V. S. Pribiag, I. N. Krivorotov, G. D. Fuchs, P. M. Braganca, O. Ozatay, J. C. Sankey, D. C. Ralph, and R. A. Buhrman, Magnetic vortex oscillator driven by d.c. spin-polarized current, Nat. Phys. **3**, 498 (2007).

[30] X. Z. Yu, D. Morikawa, K. Nakajima, K. Shibata, N. Kanazawa, T. Arima, N. Nagaosa, and Y. Tokura, Motion tracking of 80-nm-size skyrmions upon directional current injections, Sci. Adv. **6**, eaaz9744 (2020).

[31] J. Zázvorka, F. Jakobs, D. Heinze, N. Keil, S. Kromin, S. Jaiswal, K. Litzius, G. Jakob, P. Virnau, D. Pinna, K. Everschor-Sitte, L. Rózsa, A. Donges, U. Nowak, and M. Kläui, Thermal skyrmion diffusion used in a reshuffler device, Nat. Nanotechnol. **14**, 658 (2019).

[32] J. Sampaio, V. Cros, S. Rohart, A. Thiaville, and A. Fert, Nucleation, stability and current-induced motion of isolated magnetic skyrmions in nanostructures, Nat. Nanotechnol. **8**, 839 (2013).

[33] N. Nagaosa and Y. Tokura, Topological properties and dynamics of magnetic skyrmions, Nat. Nanotechnol. **8**, 899 (2013).

[34] H. G. Bauer, M. Sproll, C. H. Back, and G. Woltersdorf, Vortex Core Reversal Due to Spin Wave Interference, Phys. Rev. Lett. **112**, 077201 (2014).

[35] R. Tomasello, M. Ricci, P. Burrascano, V. Puliafito, M. Carpentieri, and G. Finocchio, Electrical detection of single magnetic skyrmion at room temperature, AIP Adv. **7**, 056022 (2017).

[36] M. Kuepferling, S. Zullino, A. Sola, B. Van De Wiele, G. Durin, M. Pasquale, K. Rott, G. Reiss, and G. Bertotti, Vortex dynamics in Co-Fe-B magnetic tunnel junctions in presence of defects, J. Appl. Phys. **117**, 17E107 (2015).

[37] X. S. Wang and X. R. Wang, Thermodynamic theory for thermal-gradient-driven domain-wall motion, Phys. Rev. B **90**, 014414 (2014).

[38] G. Tatara, Thermal vector potential theory of magnon-driven magnetization dynamics, Phys. Rev. B **92**, 064405 (2015).

[39] B. A. Ivanov and C. E. Zaspel, Gyrotropic mode frequency of vortex-state permalloy disks, J. Appl. Phys. **95**, 7444 (2004).

[40] K. Yu. Guslienko, X. F. Han, D. J. Keavney, R. Divan, and S. D. Bader, Magnetic Vortex Core Dynamics in Cylindrical Ferromagnetic Dots, Phys. Rev. Lett. **96**, 067205 (2006).

[41] See Supplemental Material at http://link.aps.org/supplemental/ 10.1103/PhysRevB.107.L100409 for further details on sample preparation, experimental details on the used imaging methods, finite element modelling of the temperature landscape, and a detailed description of the forces acting upon the vortex core within the framework of the Thiele equation (also see Refs. [38,51–57] therein).

[42] K. Yu. Guslienko, B. A. Ivanov, V. Novosad, Y. Otani, H. Shima, and K. Fukamichi, Eigenfrequencies of vortex state excitations in magnetic submicron-size disks, J. Appl. Phys. **91**, 8037 (2002).

[43] D. Suess, A. Bachleitner-Hofmann, A. Satz, H. Weitensfelder, C. Vogler, F. Bruckner, C. Abert, K. Prügl, Jürgen Zimmer, C. Huber, S. Luber, W. Raberg, T. Schrefl, and H. Brückl, Topologically protected vortex structures to realize low-noise magnetic sensors, arXiv:1712.07061.

[44] B. Van Waeyenberge, A. Puzic, H. Stoll, K. W. Chou, T. Tyliszczak, R. Hertel, M. Fähnle, H. Brückl, K. Rott, G. Reiss, I. Neudecker, D. Weiss, C. H. Back, and G. Schütz, Magnetic vortex core reversal by excitation with short bursts of an alternating field, Nature (London) **444**, 461 (2006).

[45] S. Sugimoto, Y. Fukuma, S. Kasai, T. Kimura, A. Barman, and Y. Otani, Dynamics of Coupled Vortices in a Pair of Ferromagnetic Disks, Phys. Rev. Lett. **106**, 197203 (2011).

[46] B. Krüger, A. Drews, M. Bolte, U. Merkt, D. Pfannkuche, and G. Meier, Harmonic oscillator model for current- and field-driven magnetic vortices, Phys. Rev. B **76**, 224426 (2007).

[47] M. Kuepferling, F. Garcia-Sanchez, T. Boehnert, R. Ferreira, R. Dutra, R. L. Sommer, and M. Pasquale, Influence of thermal gradients on the vortex dynamics in CoFeB MTJs, in *2017 IEEE International Magnetics Conference (INTERMAG)* (IEEE, Dublin, Ireland, 2017), p. 1.

[48] L. Bretzner and T. Lindeberg, Feature tracking with automatic selection of spatial scales, Comput. Vision Image Understanding **71**, 385 (1998).

[49] A. V. Chumak, A. A. Serga, and B. Hillebrands, Magnonic crystals for data processing, J. Phys. D **50**, 244001 (2017).

[50] A. Mahmoud, F. Ciubotaru, F. Vanderveken, A. V. Chumak, S. Hamdioui, C. Adelmann, and S. Cotofana, Introduction to spin wave computing, J. Appl. Phys. **128**, 161101 (2020).

[51] T. S. Machado, T. G. Rappoport, and L. C. Sampaio, Vortex core magnetization dynamics induced by thermal excitation, Appl. Phys. Lett. **100**, 112404 (2012).

[52] William Fuller Jr. Brown, Thermal fluctuations of fine ferromagnetic particles, IEEE Trans. Magn. **15**, 1196 (1979).

[53] P. J. Van Zwol, D. F. Vles, W. P. Voorthuijzen, M. Péter, H. Vermeulen, W. J. Van Der Zande, J. M. Sturm, R. W.E. Van De Kruijs, and F. Bijkerk, Emissivity of freestanding membranes with thin metal coatings, J. Appl. Phys. **118**, 213107 (2015).

[54] C. Y. Ho, M. W. Ackerman, K. Y. Wu, T. N. Havill, R. H. Bogaard, R. A. Matula, S. G. Oh, and H. M. James, Electrical resistivity of ten selected binary alloy systems, J. Phys. Chem. Ref. Data **12**, 183 (1983).

[55] F. K. Dejene, J. Flipse, and B. J. van Wees, Spin-dependent Seebeck coefficients of $Ni_{80}Fe_{20}$ and Co in nanopillar spin valves, Phys. Rev. B **86**, 024436 (2012).

[56] G. M. Wysin and W. Figueiredo, Thermal vortex dynamics in thin circular ferromagnetic nanodisks, Phys. Rev. B **86**, 104421 (2012).

[57] K. M. D. Hals, A. Brataas, and G. E. W. Bauer, Thermopower and thermally induced domain wall motion in (Ga, Mn)As, Solid State Commun. **150**, 461 (2010).